Vol. 19, e190008 (2022)
doi: 10.2142/biophysico.bppb-v19.0008

Biophysics and Physicobiology
https://www.jstage.jst.go.jp/browse/biophysico/

Regular Article

Slow and temperature-compensated autonomous disassembly of KaiB–KaiC complex

Damien Simon[1,2], Atsushi Mukaiyama[1,2], Yoshihiko Furuike[1,2], Shuji Akiyama[1,2]

[1] *Research Center of Integrative Molecular Systems (CIMoS), Institute for Molecular Science, National Institutes of Natural Sciences, Okazaki, Aichi 444-8585, Japan*
[2] *Department of Functional Molecular Science, SOKENDAI (The Graduate University for Advanced Studies), Okazaki, Aichi 444-8585, Japan*

Received January 5, 2022; Accepted March 28, 2022;
Released online in J-STAGE as advance publication March 30, 2022
Edited by Eriko Nango

KaiC is the central pacemaker of the circadian clock system in cyanobacteria and forms the core in the hetero-multimeric complexes, such as KaiB–KaiC and KaiA–KaiB–KaiC. Although the formation process and structure of the binary and ternary complexes have been studied extensively, their disassembly dynamics have remained elusive. In this study, we constructed an experimental system to directly measure the autonomous disassembly of the KaiB–KaiC complex under the condition where the dissociated KaiB cannot reassociate with KaiC. At 30°C, the dephosphorylated KaiB–KaiC complex disassembled with an apparent rate of 2.1 ± 0.3 d^{-1}, which was approximately twice the circadian frequency. Our present analysis using a series of KaiC mutants revealed that the apparent disassembly rate correlates with the frequency of the KaiC phosphorylation cycle in the presence of KaiA and KaiB and is robustly temperature-compensated with a Q_{10} value of 1.05 ± 0.20. The autonomous cancellation of the interactions stabilizing the KaiB–KaiC interface is one of the important phenomena that provide a link between the molecular-scale and system-scale properties.

Key words: circadian clock, cyanobacteria, rhythm, dissociation, cross-scale causality

Significance

In both prokaryotes and eukaryotes, circadian clock proteins are assembled and frozen into highly stable hetero-multimeric complexes at night, but they are disassembled autonomously at dawn to terminate internal biological night. In this study, we experimentally determined the time scale and temperature dependence of the autonomous disassembly of the KaiB–KaiC complex, one of the major clock-protein complexes in the cyanobacterial circadian clock system. Our results clearly demonstrate that the timing of KaiB release from KaiC and its temperature dependence are governed by the structure and physicochemical state of KaiC.

Introduction

In cells crowded with an astronomical number of biomolecules, a variety of enzymes function in a coordinated manner while autonomously exchanging energy and information across multiple dimensions of time, space, concentration, and structure. This autonomy sometimes becomes obvious at cellular or even higher levels, as seen in ordered patterns and shapes of plants and animals [1-3] or rhythmic phenomena that repeat in a constant temporal order [4-6].

Protein complexes are one of the molecular bases for the such autonomous control, and thus it is important to describe

Corresponding author: Shuji Akiyama, Institute for Molecular Science, 38 Nishigo-Naka, Myodaiji, Okazaki, Aichi 444-8585, Japan. ORCID iD: https://orcid.org/0000-0002-7184-189X, e-mail: akiyamas@ims.ac.jp

their dynamics from birth (assembly) to death (disassembly). The assembly dynamics of the protein complexes are greatly influenced by factors that determine the probability of encounter, such as effective concentration and spatial localization of pre-assembled components [7,8]. On the other hand, the disassembly is driven mainly by intra-complex circumstances such as structure and physicochemical state [9,10], and thus inherent properties of the disassembly dynamics may even affect the characteristics of higher-order systems [11]. While research on the formation and structure of the protein complexes tends to take precedence, research on those disassembly phenomena tends to attract limited attention and lag behind. However, studies on the macromolecular complexes in terms of those disassembly or depolymerization are important as shown in many examples [12,13], because they can provide a link between the molecular-scale and system-scale properties.

Circadian clocks are 24-h cyclic systems and thus need to be studied in terms of both assembly and disassembly of clock-protein complexes. Although clock proteins themselves are not universally conserved [14], the formation of the clock-protein complexes from dusk to night and their dissociation from dawn to daytime are common to a wide variety of species ranging from bacteria to mammals [4,5,15].

The circadian clock of cyanobacterium *Synechococcus elongatus* PCC 7942 is the simplest of such systems known today, and its core oscillator consists of three kinds of the clock proteins, KaiA, KaiB, and KaiC [16]. KaiC is a protein composed of tandemly replicated N-terminal (CI) domain and C-terminal (CII) domain [17], and binds an ATP molecule in every CI–CI and CII–CII interface to form a double-ring hexamer (Figure 1A). Assembly and disassembly cycle of the Kai oscillator can be reconstituted even *in vitro* by incubating KaiC in the presence of KaiA, KaiB, and ATP [18]. In the daytime phase, KaiA binds a C-terminal tail of KaiC and promotes auto-phosphorylation of S431 and T432 in the CII domain of KaiC (Figure 1B). Previous studies have shown that the phosphor-transfer reaction in KaiC advances in a sequential manner [19,20]: ST → SpT → pSpT → pST → ST, where S, pS, T and pT represent S431, phosphorylated S431, T432, and phosphorylated T432, respectively. At dusk (Figure 1B), KaiB binds the CI domain of phosphorylated KaiCs such as KaiC-pSpT and KaiC-pST to form a KaiB–KaiC complex [19,21]. In night time (Figure 1B), KaiA is recruited to KaiB interacting with the CI domain of KaiC and then trapped in a deactivated morphology as a KaiA–KaiB–KaiC complex [22,23]. It is hypothesized that the KaiB–KaiC interface in the night complex is destabilized before and/or after the process of KaiC auto-dephosphorylation from KaiC-pST to KaiC-ST [24], and the KaiA–KaiB–KaiC complex is completely dissociated into respective components at dawn [25] (Figure 1B).

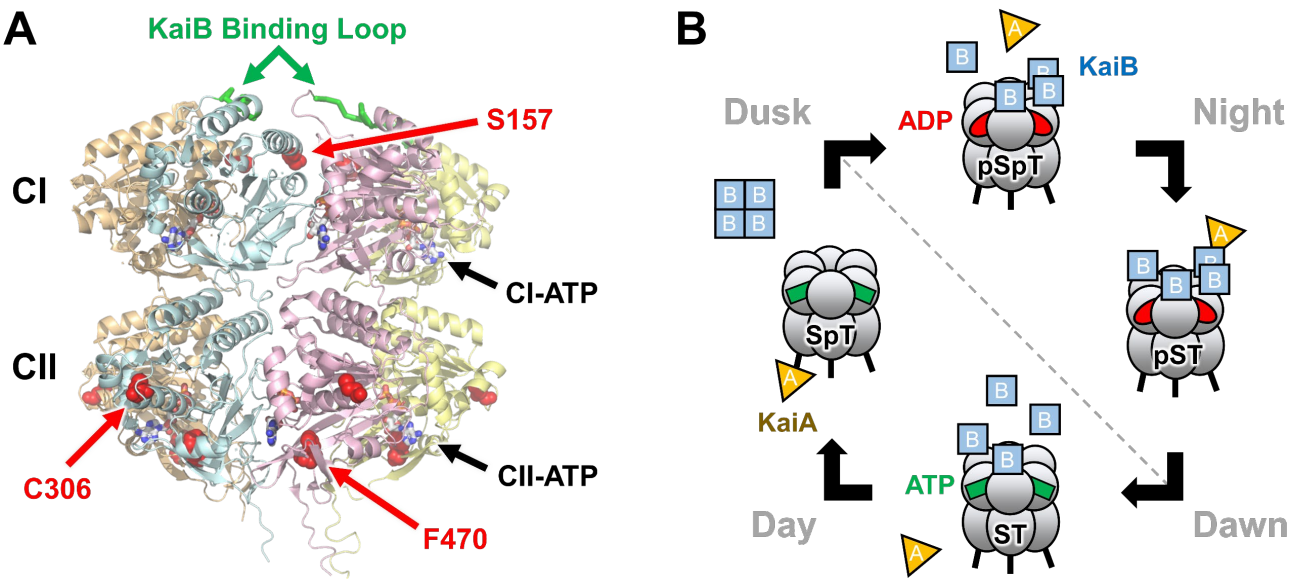

Figure 1 KaiC as the core of the circadian clock system in cyanobacteria. (A) Mutation sites mapped on the crystal structure of KaiC with tandemly replicated N-terminal (CI) and C-terminal (CII) domains [17]. Nucleotide molecules such as ATP and ADP are bound in every CI–CI and CII–CII interface to form the double-ring hexamer. (B) Schematic representation of the rhythmic assembly and disassembly in the cyanobacterial circadian clock system during the day-night cycle [22]. An orange triangle, a sky-blue box, a green box, and a red ellipsoid corresponds to KaiA dimer, KaiB monomer, CI-ATP, and CI-ADP, respectively.

To date, the structures [22,23] and formation kinetics [15,26-28] of the KaiB–KaiC and KaiA–KaiB–KaiC complexes have been studied in detail using a variety of physicochemical techniques. The tetrameric KaiB monomerizes and then

undergoes a fold switch to become an activated form of KaiB [26]. The activated KaiB is considered to bind preferentially the CI domain in a post-hydrolysis state [22,23]. On the other hand, the disassembly process of these complexes is poorly characterized. Whereas KaiB bound to KaiC interacts strongly and specifically with KaiA [29], the interaction between free KaiB and KaiA is not strong enough to accumulate the KaiA–KaiB complex in the circadian time scale [27,30]. Hence, the process of actively disrupting the specific interaction between KaiB and KaiC is the key to elucidating the disassembly dynamics of the KaiB–KaiC and KaiA–KaiB–KaiC complexes. Experimental determination of its time scale and properties is of particular importance for understanding the mechanism by which the Kai oscillator resets the night history and turns the cyclic reaction (Figure 1B).

In this study, we observed the dissociation process of KaiB from the KaiB–KaiC complex and estimated the timescale of the autonomous KaiB–KaiC disassembly. We also carried out measurements using a series of KaiC mutants with shorter or longer period length to investigate a potential relationship between the KaiB–KaiC disassembly and the frequency of the Kai oscillator. Furthermore, we investigated the temperature dependence of the apparent rate of the KaiB–KaiC disassembly. Our results suggest that the apparent rate and temperature dependence of the disassembly process of KaiB from the KaiB–KaiC complex is related to the frequency and temperature compensation of the circadian clock system in cyanobacteria.

Materials and Methods

Expression and Purification of Kai Proteins

Kai proteins were expressed as recombinant proteins using *E. coli* BL21(DE3) and purified as described previously [31].

Equilibration of KaiB‑KaiC Complexes

A mixture of equimolar amounts of KaiB and KaiC (17 μM on a monomer basis) was incubated at 30°C in a buffer containing 20 mM Tris/HCl (pH 8.0), 150 mM NaCl, 0.5 mM EDTA, 1 mM ATP, 5 mM $MgCl_2$ and 1 mM DTT, and every aliquot taken at different time points for 48 h was applied to Superdex 200 Increase 10/300 column (Cytiva) equilibrated with a buffer containing 20 mM Tris/HCl (pH 8.0), 150 mM NaCl, 0.5 mM EDTA, 1 mM ATP, 5 mM $MgCl_2$ and 1 mM DTT. Assignment of the elution peaks was conducted by sodium dodecyl sulfate polyacrylamide gel electrophoresis (SDS-PAGE) analysis of the fractionated samples.

Disassembly Experiments

In order to exchange bulk nucleotides from ATP to adenylyl-imidodiphosphate (AMP-PNP), the KaiB–KaiC complex that was pre-formed after the assembly experiments at 25°C, 30°C, or 35°C for 48 h was applied to a HiTrap Desalting column (Cytiva) equilibrated with a buffer containing 20 mM Tris/HCl (pH 8.0), 150 mM NaCl, 0.5 mM EDTA, 5 mM $MgCl_2$, 1 mM DTT, and 1mM AMP-PNP. Fractions containing the KaiB–KaiC complex were collected immediately and then incubated at 25°C, 30°C, or 35°C to initiate the disassembly reaction ($t = 0$). At every time point, an aliquot of the incubated sample was applied to Superdex 200 Increase 10/300 column (Cytiva) equilibrated with a buffer containing 20 mM Tris/HCl (pH 8.0), 150 mM NaCl, 0.5 mM EDTA, 5 mM $MgCl_2$, and 1 mM DTT.

Analysis of Size-Exclusion Chromatography Data

Elution curves were analyzed with Multipeak Fitting 2 package in Igor Pro software (WaveMetrics) and then fitted using the following equation,

$$Abs(v) = Base(v) + BC(v) + C(v) + B(v) \quad (1)$$

where $Abs(v)$ is the absorbance at 280 nm at the elution volume of v; $Base(v)$ is a cubic function of $\log(v)$ for a baseline [32]; $BC(v)$, $C(v)$, and $B(v)$ are exponentially modified Gaussian functions [33] for the elution peaks of KaiB–KaiC complexes, KaiC, and KaiB, respectively. The relative intensity of the elution peak for KaiB (I_B) was determined according to the following relationship,

$$I_B = Area_B/(Area_{BC} + Area_C + Area_B) \quad (2)$$

where $Area_{BC}$, $Area_C$, and $Area_B$ correspond to the peak areas of $BC(v)$, $C(v)$, and $B(v)$, respectively. In rare cases where $BC(v)$ and $C(v)$ were not sufficiently separated, they were analyzed together as one peak, but it should be noted that this does not affect the estimation of the I_B value.

In vitro KaiC Phosphorylation Rhythms

KaiC phosphorylation cycle was reconstructed at 25°C, 30°C, or 35°C by incubating KaiA (0.04 mg/ml), KaiB (0.04

mg/ml), and KaiC (0.2 mg/ml) in a buffer containing 20 mM Tris/HCl (pH 8.0), 150 mM NaCl, 0.5 mM EDTA, 1 mM ATP, 5 mM $MgCl_2$ and 1 mM DTT as described previously [18]. The abundance of the phosphorylated KaiC was quantified with SDS-PAGE and densitometric analysis of gel bands using LOUPE software [34].

Results

Pre-Formation of KaiB–KaiC Complexes

The binding process of KaiB and KaiC has been studied in detail [26-28], and it is known to exhibit slow binding relaxation as long as approximately 24 h [15,25]. In order to reproducibly prepare the KaiB–KaiC complex for disassembly experiments, we investigated the time required for equilibrating the formation dynamics of the KaiB–KaiC complex. KaiB and wild-type KaiC ($KaiC^{WT}$) were mixed with an equimolar ratio (17 μM on a monomer basis), and the resultant KaiB/$KaiC^{WT}$ mixture was incubated at 30°C. At every time point, an aliquot of the incubated sample was applied to size-exclusion chromatography (SEC) to observe the progress of the binding reaction. The elution curve immediately after mixing KaiB and $KaiC^{WT}$ showed two peaks eluting at 10.3 and 14.7 mL (P1 and P2 in Figure 2A). SDS-PAGE analysis of the fractionated samples indicated that the P1 and P2 corresponded to the free $KaiC^{WT}$ and KaiB, respectively (Figure 2B). The peak intensity of the free KaiB decreased with time, and concomitantly $KaiC^{WT}$ was coeluted with KaiB as the KaiB–$KaiC^{WT}$ complex at a smaller elution volume of 10.0 mL (P3 in Figure 2A and 2B). After 48 h incubation, the peaks of the KaiB–$KaiC^{WT}$ complex and free KaiB remained unchanged. Thus, the 48-h pre-incubated KaiB/KaiC mixture was used as the starting sample for the following dissociation experiments.

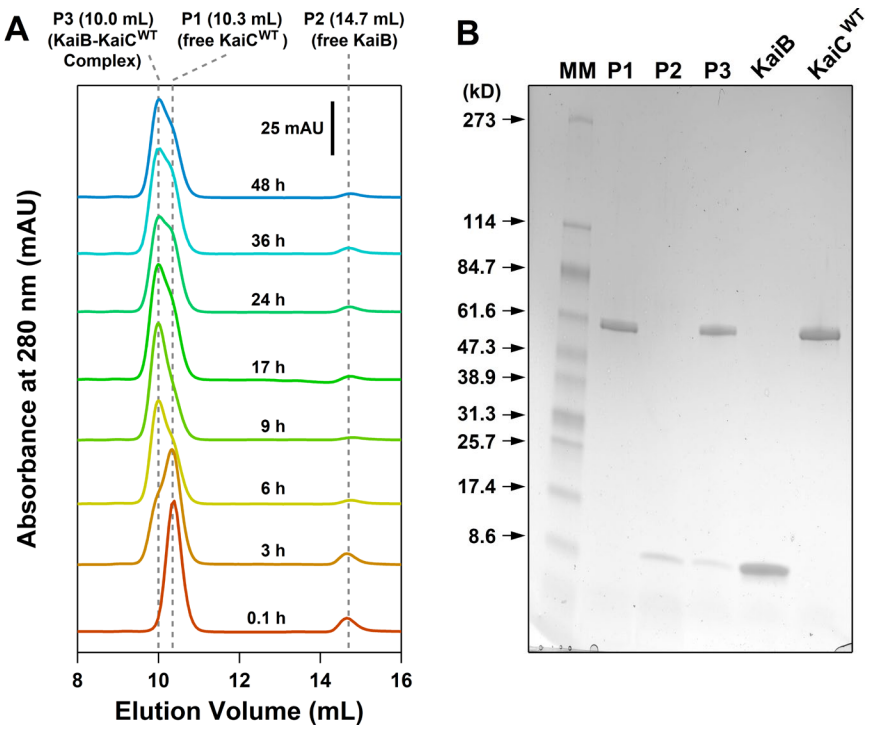

Figure 2 Formation of the KaiB–$KaiC^{WT}$ complex. (A) Elution curves of size exclusion chromatography of the mixtures containing KaiB and $KaiC^{WT}$ in an equimolar ratio (17 μM), after different incubation times at 30°C. Traces are vertically shifted for clarity of the presentation. The three dashed lines correspond to the elution volumes of the three peaks, P1, P2, and P3. (B) SDS-PAGE analysis of molecular mass markers (MM), P1, P2, P3, KaiB, and $KaiC^{WT}$.

Disassembly Kinetics of KaiB–KaiC Complex

To observe the dissociation kinetics directly, it is necessary to control the reassociation process of dissociated free KaiB into KaiC. For this purpose, the disassembly of the KaiB–$KaiC^{WT}$ complex was initiated by replacing the bulk ATP with its non-hydrolysable analogue, AMP-PNP, because KaiB is known to bind selectively to the ADP-bound state of KaiC but never to the AMP-PNP–bound state of KaiC [28,35,36].

The pre-formed KaiB–$KaiC^{WT}$ complex was subjected to an immediate (less than 10 min) buffer exchange using a

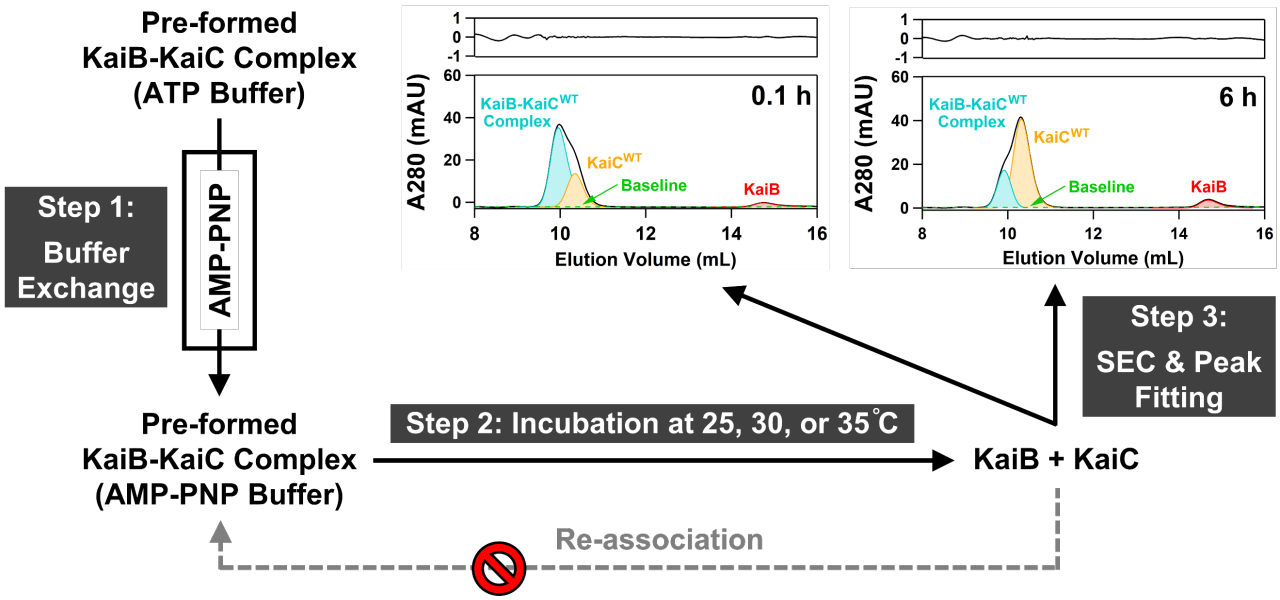

Figure 3 Schematic representation of the experimental method for tracking the disassembly dynamics of the KaiB–KaiC complex. Step 1: buffer exchange of the pre-formed KaiB–KaiC complex to replace bulk ATP to AMP-PNP. Step 2: incubation time to allow autonomous disassembly of KaiB–KaiC complex at three different temperatures. Step 3: size-exclusion chromatography (SEC) analysis of the incubated samples. Shown chromatograms are representative results of KaiC^{WT}, which were analyzed using the Eq.(1) to identify the peaks of KaiB–KaiC^{WT} complexes (sky-blue), KaiC^{WT} (orange), and KaiB (red), respectively. Upper panels of the shown chromatograms indicate residuals of the fitting analysis (see details in Materials and Methods).

desalting column equilibrated with a buffer containing AMP-PNP instead of ATP (t = 0, step 1 in Figure 3), and the resultant KaiB–KaiC^{WT} complex was incubated at 30°C (step 2 in Figure 3). At every time point, an aliquot of the buffer-exchanged sample was applied to SEC to trace the change in the association state of the KaiB–KaiC^{WT} complex (step 3 in Figure 3). Immediately after the buffer exchange (t = 0.1 h), the sample was eluted in two peaks (Figure 3). The larger peak at 10.0 mL corresponded to the KaiB–KaiC^{WT} complex, and its minor shoulder on the side of higher elution volume was derived from a small amount of free KaiC^{WT}. The smaller peak at 14.7 mL was attributed to a small amount of free KaiB. As the time proceeded (t = 6 h), the peaks of free KaiC^{WT} and KaiB became intense, while that of the KaiB–KaiC^{WT} complex became faint (Figure 3). After 36 h (Figure 4A), the peak corresponding to the KaiB–KaiC^{WT} complex remained apparently disappeared, and that of free KaiB remained unchanged. These results suggest that the buffer-exchange suppresses the recombination of dissociated free KaiB as we intended (Figure 3), and that the relaxation observed as in Figure 4A directly reflects the dissociation kinetics of the KaiB–KaiC^{WT} complex.

To estimate the apparent rate constant of the disassembly, time-course of the relative peak intensity for KaiB was fitted using the following exponential function (Figure 4B),

$$I_B(t) = I_B^{\infty} + \Delta I_B \, e^{-k_{off}^{app} t} \quad (3)$$

where $I_B(t)$ is the peak intensity of KaiB at time t, expressed as a relative value to the intensity of all peaks (details in Materials and Methods); I_B^{∞} is the peak intensity of KaiB at infinite time; ΔI_B represents the amplitude of the exponential phase; and k_{off}^{app} is the apparent rate constant of the disassembly reaction. The resultant k_{off}^{app} value for the KaiB–KaiC^{WT} complex was $8.6 \pm 1.4 \times 10^{-2}$ h^{-1} (2.1 ± 0.3 d^{-1}).

To test whether the dissociation rate is related to the stability of the KaiB–KaiC complex, we performed the same experiment using a KaiC-pSpT–mimicking S431D/T432E KaiC mutant (KaiC^{DE}) that is known to show a significantly higher affinity for KaiB [19,20,28,36]. Astonishingly, the disassembly kinetics of the KaiB–KaiC^{DE} complex lasted for over 2 weeks (Figure 4B) with k_{off}^{app} of $5.6 \pm 0.3 \times 10^{-3}$ h^{-1} (0.13 ± 0.1 d^{-1}). This result suggests that the slowness of the disassembly kinetics is one of the factors contributing to the higher affinity of KaiB for KaiC. Considering that KaiC^{WT} in the pre-formed KaiB–KaiC^{WT} complex was almost completely dephosphorylated, the dual phosphorylation of S431 and T432 slowed down the KaiB–KaiC disassembly by approximately 20-fold.

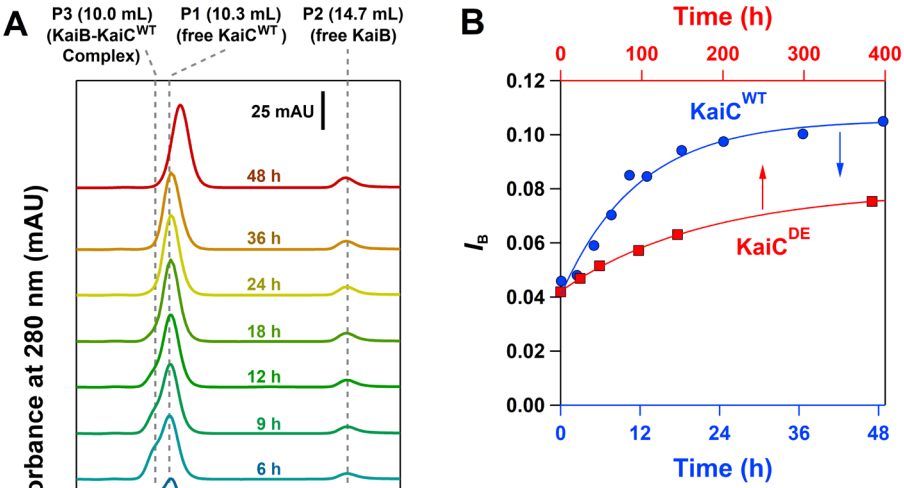

Figure 4 Disassembly of the KaiB–KaiC^{WT} complex under the condition where the dissociated KaiB cannot reassociate with KaiC. (A) Time evolution of SEC chromatograms for the pre-formed KaiB–KaiC^{WT} complex. Each trace was vertically shifted for clarity of the presentation. The three dashed lines correspond to the elution volumes of the three peaks, P1, P2, and P3. (B) Disassembly kinetics of the KaiB–KaiC^{WT} (blue) and KaiB–KaiC^{DE} (red) complexes. Relative peak intensity for KaiB (I_B) was estimated using Eq.(2) and analyzed using Eq.(3) (solid lines). The apparent disassembly rate constants (k_{off}^{app}) for KaiB–KaiC^{WT} and KaiB–KaiC^{DE} complexes were $8.6 \pm 1.4 \times 10^{-2}$ h^{-1} (2.1 ± 0.3 d^{-1}) and $5.6 \pm 0.3 \times 10^{-3}$ h^{-1} (0.13 ± 0.1 d^{-1}), respectively.

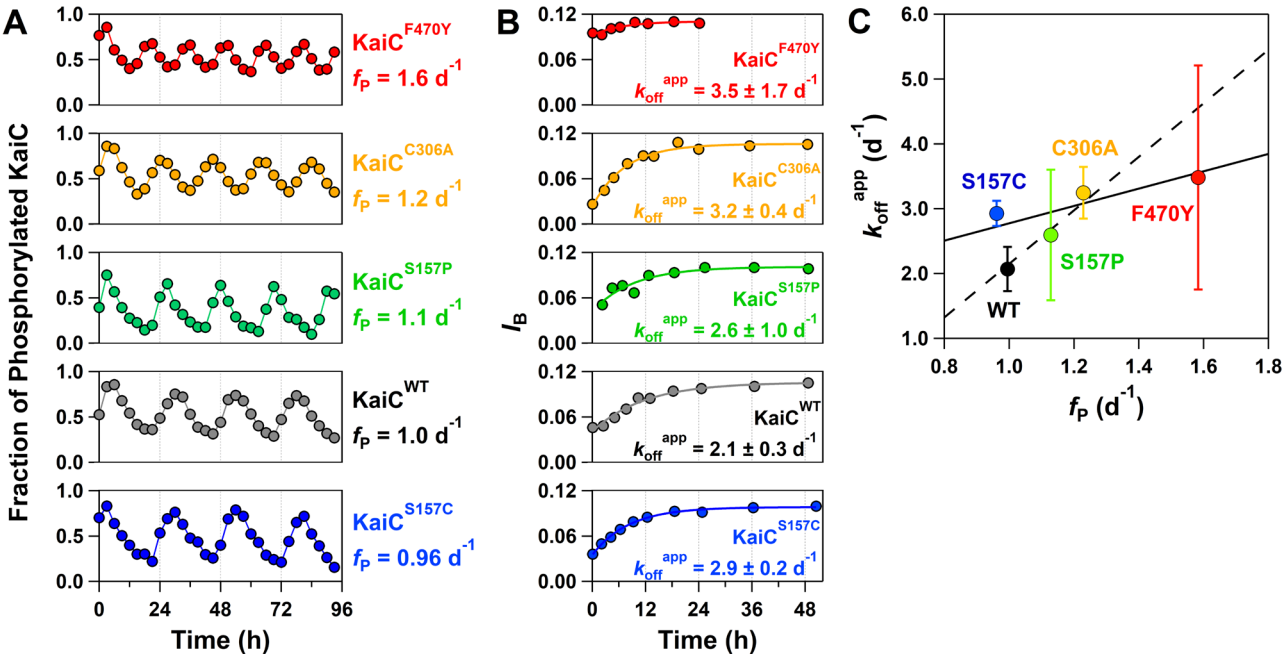

Figure 5 Analysis of the KaiC mutants at 30°C. (A) *In vitro* phosphorylation cycles of KaiC^{WT} and its mutants in the presence of KaiA (0.04 mg/mL) and KaiB (0.04 mg/mL). The cycle frequency (f_P) determined according to the previous report [34] is shown on the right side of each panel. (B) Time-courses of relative peak intensity for KaiB (I_B) during the disassembly of the KaiB–KaiC complexes. Apparent disassembly rate constants (k_{off}^{app}) were determined by fitting Eq.(3) to the data (solid lines). (C) Correlation plot between k_{off}^{app} and f_P. Linear regressions with (solid line) and without (dashed line) KaiC^{S157C} resulted in correlation coefficients of 0.57 and 0.96, respectively.

Period-Mutants Analysis

To investigate potential effects of the KaiB–KaiC disassembly on the KaiC phosphorylation cycle, we conducted the experiments using a series of KaiC mutants exhibiting a higher or lower oscillatory frequency than KaiC^{WT}. As shown in Figure 5A, while a S157C substitution caused a slight decrease in the frequency of the phosphorylation cycle (f_P = period / 24 = 0.96 d^{-1}), other substitutions such as S157P (1.1 d^{-1}), C306A (1.2 d^{-1}), and F470Y (1.6 d^{-1}) resulted in the increase in the f_P value [37-39]. These mutants were pre-incubated with KaiB for 48 h and then analyzed using the same protocol as described in Figure 3.

The disassembly dynamics of the high-f_P KaiC mutants were systematically faster than that of KaiC^{WT} (Figure 5B). For the dataset consisting of the high-f_P KaiC mutants and KaiC^{WT}, the increasing order of the k_{off}^{app} value matched the increasing order of the f_P value in the presence of KaiA and KaiB (Figure 5A and 5B). On the other hand, the k_{off}^{app} value for the low-f_P mutant, KaiC^{S157C} (2.9 ± 0.2 d^{-1}), was larger than that of KaiC^{WT} (2.1 ± 0.3 d^{-1}). A data point of KaiC^{S157C} in the k_{off}^{app}–f_P plot (Figure 5C) appeared to deviate from the potential correlation suggested by the high-f_P mutants (dashed line in Figure 5C, r = 0.96). Nevertheless, the data set consisting of all mutants and KaiC^{WT} suggested a certain correlation between the k_{off}^{app} and f_P values (solid line in Figure 5C, r = 0.57).

Temperature Dependence of the Disassembly Kinetics of KaiB–KaiC Complex

Temperature insensitivity of the oscillatory frequency is one of the unique properties of the circadian clocks [40] as distinguished from other chemical oscillators showing temperature sensitivity [41]. As observed previously [18], the f_P values of KaiC^{WT} were insensitive to the temperature (Figure 6A). The Q_{10} value of f_P (Q_{10}^{fp}) was estimated to be 1.16 ± 0.01 (Figure 6C), which was nearly consistent with 1.09 ± 0.01 in the previous report [34]. To investigate the temperature dependence of the disassembly dynamics, the KaiB–KaiC^{WT} complexes that were pre-formed at 25°C, 30°C, and 35°C for 48 h were buffer exchanged and then incubated at three corresponding temperatures at 25°C, 30°C, and 35°C, respectively (Figure 3). While the amplitude (ΔI_B) of the exponential relaxation increased as the temperature increased, the relative peak intensity after the relaxation (I_B^{∞}) was nearly unaffected by the temperature change (Figure 5B). Furthermore, k_{off}^{app} of the KaiB–KaiC^{WT} complex was temperature-compensated with the Q_{10}^{koff} value of 1.05 ± 0.20 (Figure 5C). These results imply that the dissociation process of the KaiB–KaiC complex is somehow related to the temperature compensatory nature of the KaiC phosphorylation cycle.

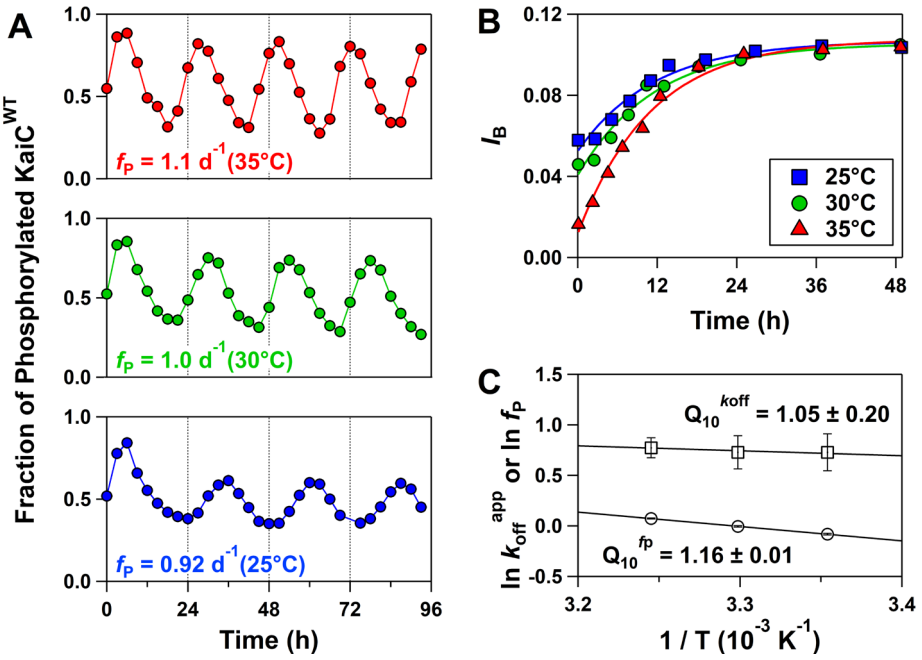

Figure 6 Temperature-insensitive disassembly of the KaiB–KaiC^{WT} complex. (A) KaiC^{WT} phosphorylation cycle in the presence of KaiA (0.04 mg/mL) and KaiB (0.04 mg/mL) at 25°C, 30°C and 35°C. (B) Time-courses of relative peak intensity for KaiB (I_B) during the disassembly of the KaiB–KaiC^{WT} complex at 25°C, 30°C and 35°C. Apparent disassembly rate constants (k_{off}^{app}) were determined by fitting Eq.(3) to the data (solid lines). (C) Arrhenius plot analysis of k_{off}^{app} (boxes) and phosphorylation cycle frequency (f_P, circles). The activation energy, which was determined by linear regression (solid lines), was converted to the Q_{10} value at 303 K as described previously [34].

According to Eq. (2), the initial I_B value immediately after solution exchange is a kind of parameter that reflects the magnitude of the equilibrium dissociation constant of the KaiB–KaiC complex in the presence of ATP. The fact that the initial I_B value decreased in a temperature-dependent manner (Fig. 6B) while k_{off}^{app} was temperature-insensitive implies a view of temperature-sensitive assembly and temperature-insensitive disassembly of the KaiB–KaiC^{WT} complex.

Discussion

The time scale for dissociation of protein complexes varies widely from milliseconds to hours, depending on their structures, internal states, and functional requirements. The apparent disassembly rate of the KaiB–KaiC complex observed in this study seems to belong to the slowest part of this diversity. Microtubules are disassembled quickly with a rate of 113 s^{-1} at 30°C [42]. Dimerized G-protein–coupled receptor undergoes the monomerization with a rate of 11 s^{-1} at 37°C [43]. Barbed and pointed ends of ADP-actin filaments are depolymerized at 22°C with rates of 7.2 and 0.27 s^{-1}, respectively [44]. The dissociation rates of end-binding proteins Arp2/3 complex and capping protein from the actin filament are determined to be 0.048 and 0.58 s^{-1}, respectively [45]. Bovine 26S proteasome is one of the slower examples, which dissociates into core 20S proteasome and regulatory complex with a rate of 0.744 h^{-1} at 25°C [46]. Tetramer-to-dimer dissociation of human hemoglobin advances very slowly at 30°C with a rate of 0.315 h^{-1} (7.56 d^{-1}) [47]. The steady-state ATPase activity of KaiC is approximately 0.5 h^{-1} (12 d^{-1}) at 30°C [37,39,48]. Although certain attention should be paid in making these comparisons due to the differences in measurement temperatures and analysis methods, the release of KaiB from the KaiB–KaiC complex is the quite slow phenomenon ($8.6 \pm 1.4 \times 10^{-2}$ h^{-1} (2.1 ± 0.3 d^{-1}) ~ $5.6 \pm 0.3 \times 10^{-3}$ h^{-1} (0.13 ± 0.1 d^{-1})) compared to various assembly-disassembly systems including the circadian clock of cyanobacteria. The remarkably small k_{off}^{app} value recalls a possibility that a slow change in the internal states of KaiC is the rate-liming process for the spontaneous disassembly of the KaiB–KaiC complex.

The cyanobacterial circadian clock is the unique system in which causality is established between molecule- and system-levels [37,39,48]: if the ATPase activity of KaiC is doubled by amino acid substitutions, the f_P value in the presence of KaiA and KaiB is also doubled. In the present study, we investigated the molecule-system correlation from the viewpoint of the autonomous KaiB dissociation. For the dataset consisting of the high-f_P KaiC mutants and KaiC^{WT}, we observed the fine correlation between the k_{off}^{app} and f_P values ($r = 0.96$, dashed line in Figure. 5C). The molecule-system correlation of the KaiB–KaiC disassembly was confirmed not only in terms of the rate of the reaction (Figure 5C) but also in terms of its robustness to temperature changes (Figure 6C). These observations suggest that the autonomous dissociation of the KaiB–KaiC complex is one of the important phenomena that provide a causal link between the circadian clock system and its constituent molecules.

In this regard, the fact that KaiC^{S157C} exhibited the larger k_{off}^{app} value than KaiC^{WT} was unexpected (Figure 5B). When the low-f_P KaiC^{S157C} was included, the correlation coefficient of the k_{off}^{app}–f_P plot decreased from 0.96 to 0.57 (Figure 5C). This may be partly due to the relative bias in the k_{off}^{app} errors among KaiC^{WT} and the mutants. In addition, there are two possible explanations. The first is a circumstance specific to the 157th position in KaiC, where the amino acid substitution was introduced. According to the crystal structure of the KaiB–KaiC complex [22], S157 is located in close proximity to the KaiB binding loop (116–123) of KaiC at a distance of 8–9 Å (Figure 1A). Furthermore, S157 is known as the key residue that indirectly regulates positioning of a lytic water molecule for CI-ATP [37]. However, the well-correlated data point of KaiC^{S157P} (Figure 5C) makes it unlikely that the reason is specific to the 157th position. The second is the additional effect of KaiA on the dissociation of the KaiB–KaiC complex. According to the previous studies [27,49], KaiA can indirectly lower the affinity of KaiC for KaiB by binding to the C-terminus of KaiC. It may be possible that this indirect effect of KaiA is partially inhibited by the S157C mutation, resulting in the decrease in the f_P value of KaiC^{S157C}. In any case, further studies in terms of the KaiB–KaiC disassembly are needed to explain the poor molecule-system correlation in KaiC^{S157C}.

The wide dynamic range of k_{off}^{app} ranging from 0.13 to 2.1 d^{-1} provides the molecular basis for the robust and rhythmic regulation of the KaiB–KaiC affinity. The dual phosphorylation in the CII domain reduced k_{off}^{app} by approximately 20-fold (Figure 4B), but the KaiB binding loop is located in the CI domain of KaiC [22,23] (Figure 1A). This result indicates that the wide dynamic range of k_{off}^{app} is derived from the delicate allostery between the CI and CII domains. In fact, the k_{off}^{app}–f_P correlation has been confirmed not only for the CII-domain mutants such as KaiC^{C306A} and KaiC^{F470Y}, but also for the CI-domain mutant such as KaiC^{S157P} (Figure 5C). It is the internal state of KaiC, such as bound nucleotides, phosphorylation, and the quaternary structure of the hexamer, that underlies the slow and temperature-compensated dissociation reaction of KaiB, and the detailed mechanism will be hidden in the coupling between the CI and CII domains. We will continue our experiments with improved time resolution and number of sampling points in order to extract information about the cooperativity of neighboring bound-KaiBs and/or the internal states of KaiC.

Conclusion

In this study, we investigated the autonomous disassembly of the KaiB–KaiC complex. The dephosphorylated KaiB–KaiC complex disassembled with the apparent rate of 2.1 ± 0.3 d^{-1} at 30°C. The disassembly dynamics was decelerated by approximately 20-fold by the dual phosphorylation of S431 and T432 in KaiC. Potential causality between the KaiB–KaiC disassembly and the phosphorylation cycle was confirmed in terms of both the reactions rates and their robust temperature compensation.

Conflict of Interest

The authors declare that no competing interests exist.

Author Contributions

D.S., A.M., and S.A. designed the research. D.S. conducted biochemical experiments with supports from A.M. and Y.F. S.A. and D.S. wrote the paper with inputs from all the authors.

Acknowledgments

This study was supported by Grants-in-Aid for Scientific Research (17H06165 to S.A.; 19K16061 to Y.F.; and 18K06171 to A.M.).

References

[1] Dhoot, G. K., Gustafsson, M. K., Ai, X., Sun, W., Standiford, D. M., Emerson, C. P., Jr. Regulation of Wnt signaling and embryo patterning by an extracellular sulfatase. Science 293, 1663-1666 (2001). https://doi.org/10.1126/science.293.5535.1663

[2] Kageyama, R., Niwa, Y., Shimojo, H., Kobayashi, T., Ohtsuka, T. Ultradian oscillations in notch signaling regulate dynamic biological events. Curr. Top. Dev. Biol. 92, 311-331 (2010). https://doi.org/10.1016/S0070-2153(10)92010-3

[3] Kondo, S., Miura, T. Reaction-diffusion model as a framework for understanding biological pattern formation. Science 329, 1616-1620 (2010). https://doi.org/10.1126/science.1179047

[4] Matsuda, M., Hayashi, H., Garcia-Ojalvo, J., Yoshioka-Kobayashi, K., Kageyama, R., Yamanaka, Y., et al. Species-specific segmentation clock periods are due to differential biochemical reaction speeds. Science 369, 1450-1455 (2020). https://doi.org/10.1126/science.aba7668

[5] Partch, C. L. Orchestration of circadian timing by macromolecular protein assemblies. J. Mol. Biol. 432, 3426-3448 (2020). https://doi.org/10.1016/j.jmb.2019.12.046

[6] Buhusi, C. V., Meck, W. H. What makes us tick? Functional and neural mechanisms of interval timing. Nat. Rev. Neurosci. 6, 755-765 (2005). https://doi.org/10.1038/nrn1764

[7] Cohen, S. E., Erb, M. L., Selimkhanov, J., Dong, G., Hasty, J., Pogliano, J., et al. Dynamic localization of the cyanobacterial circadian clock proteins. Curr. Biol. 24, 1836-1844 (2014). https://doi.org/10.1016/j.cub.2014.07.036

[8] Ryu, J. K., Min, D., Rah, S. H., Kim, S. J., Park, Y., Kim, H., et al. Spring-loaded unraveling of a single SNARE complex by NSF in one round of ATP turnover. Science 347, 1485-1489 (2015). https://doi.org/10.1126/science.aaa5267

[9] Nangle, S. N., Rosensweig, C., Koike, N., Tei, H., Takahashi, J. S., Green, C. B., et al. Molecular assembly of the period-cryptochrome circadian transcriptional repressor complex. eLife 3, e03674 (2014). https://doi.org/10.7554/eLife.03674

[10] Hale, C. A., Meinhardt, H., de Boer, P. A. Dynamic localization cycle of the cell division regulator MinE in *Escherichia coli*. EMBO J. 20, 1563-1572 (2001). https://doi.org/10.1093/emboj/20.7.1563

[11] Gwon, Y., Maxwell, B. A., Kolaitis, R. M., Zhang, P., Kim, H. J., Taylor, J. P. Ubiquitination of G3BP1 mediates stress granule disassembly in a context-specific manner. Science 372, eabf6548 (2021). https://doi.org/10.1126/science.abf6548

[12] Schütz, S., Michel, E., Damberger, F. F., Oplová, M., Peña, C., Leitner, A., et al. Molecular basis for disassembly of an importin:ribosomal protein complex by the escortin Tsr2. Nat. Commun. 9, 3669 (2018). https://doi.org/10.1038/s41467-018-06160-x

[13] Tanaka, K., Takeda, S., Mitsuoka, K., Oda, T., Kimura-Sakiyama, C., Maéda, Y., et al. Structural basis for cofilin

binding and actin filament disassembly. Nat. Commun. 9, 1860 (2018). https://doi.org/10.1038/s41467-018-04290-w
[14] Saini, R., Jaskolski, M., Davis, S. J. Circadian oscillator proteins across the kingdoms of life: Structural aspects. BMC Biol. 17, 13 (2019). https://doi.org/10.1186/s12915-018-0623-3
[15] Akiyama, S., Nohara, A., Ito, K., Maéda, Y. Assembly and disassembly dynamics of the cyanobacterial periodosome. Mol. Cell 29, 703-716 (2008). https://doi.org/10.1016/j.molcel.2008.01.015
[16] Ishiura, M., Kutsuna, S., Aoki, S., Iwasaki, H., Andersson, C. R., Tanabe, A., et al. Expression of a gene cluster kaiABC as a circadian feedback process in cyanobacteria. Science 281, 1519-1523 (1998). https://doi.org/10.1126/science.281.5382.1519
[17] Pattanayek, R., Williams, D. R., Pattanayek, S., Xu, Y., Mori, T., Johnson, C. H., et al. Analysis of KaiA-KaiC protein interactions in the cyano-bacterial circadian clock using hybrid structural methods. EMBO J. 25, 2017-2028 (2006). https://doi.org/10.1038/sj.emboj.7601086
[18] Nakajima, M., Imai, K., Ito, H., Nishiwaki, T., Murayama, Y., Iwasaki, H., et al. Reconstitution of circadian oscillation of cyanobacterial KaiC phosphorylation in vitro. Science 308, 414-415 (2005). https://doi.org/10.1126/science.1108451
[19] Nishiwaki, T., Satomi, Y., Kitayama, Y., Terauchi, K., Kiyohara, R., Takao, T., et al. A sequential program of dual phosphorylation of KaiC as a basis for circadian rhythm in cyanobacteria. EMBO J. 26, 4029-4037 (2007). https://doi.org/10.1038/sj.emboj.7601832
[20] Rust, M. J., Markson, J. S., Lane, W. S., Fisher, D. S., O'Shea, E. K. Ordered phosphorylation governs oscillation of a three-protein circadian clock. Science 318, 809-812 (2007). https://doi.org/10.1126/science.1148596
[21] Chang, Y. G., Tseng, R., Kuo, N. W., LiWang, A. Rhythmic ring-ring stacking drives the circadian oscillator clockwise. Proc. Natl. Acad. Sci. U.S.A. 109, 16847-16851 (2012). https://doi.org/10.1073/pnas.1211508109
[22] Tseng, R., Goularte, N. F., Chavan, A., Luu, J., Cohen, S. E., Chang, Y. G., et al. Structural basis of the day-night transition in a bacterial circadian clock. Science 355, 1174-1180 (2017). https://doi.org/10.1126/science.aag2516
[23] Snijder, J., Schuller, J. M., Wiegard, A., Lossl, P., Schmelling, N., Axmann, I. M., et al. Structures of the cyanobacterial circadian oscillator frozen in a fully assembled state. Science 355, 1181-1184 (2017). https://doi.org/10.1126/science.aag3218
[24] Murayama, Y., Mukaiyama, A., Imai, K., Onoue, Y., Tsunoda, A., Nohara, A., et al. Tracking and visualizing the circadian ticking of the cyanobacterial clock protein KaiC in solution. EMBO J. 30, 68-78 (2011). https://doi.org/10.1038/emboj.2010.298
[25] Kageyama, H., Nishiwaki, T., Nakajima, M., Iwasaki, H., Oyama, T., Kondo, T. Cyanobacterial circadian pacemaker: Kai protein complex dynamics in the KaiC phosphorylation cycle in vitro. Mol. Cell 23, 161-171 (2006). https://doi.org/10.1016/j.molcel.2006.05.039
[26] Chang, Y. G., Cohen, S. E., Phong, C., Myers, W. K., Kim, Y. I., Tseng, R., et al. Circadian rhythms. A protein fold switch joins the circadian oscillator to clock output in cyanobacteria. Science 349, 324-328 (2015). https://doi.org/10.1126/science.1260031
[27] Chow, G. K., Chavan, A. G., Heisler, J. C., Chang, Y. G., LiWang, A., Britt, R. D. Monitoring protein-protein interactions in the cyanobacterial circadian clock in real time via electron paramagnetic resonance spectroscopy. Biochemistry 59, 2387-2400 (2020). https://doi.org/10.1021/acs.biochem.0c00279
[28] Mukaiyama, A., Furuike, Y., Abe, J., Koda, S. I., Yamashita, E., Kondo, T., et al. Conformational rearrangements of the C1 ring in KaiC measure the timing of assembly with KaiB. Sci. Rep. 8, 8803 (2018). https://doi.org/10.1038/s41598-018-27131-8
[29] Iwasaki, H., Taniguchi, Y., Ishiura, M., Kondo, T. Physical interactions among circadian clock proteins KaiA, KaiB and KaiC in cyanobacteria. EMBO J. 18, 1137-1145 (1999). https://doi.org/10.1093/emboj/18.5.1137
[30] Mutoh, R., Mino, H., Murakami, R., Uzumaki, T., Takabayashi, A., Ishii, K., et al. Direct interaction between KaiA and KaiB revealed by a site-directed spin labeling electron spin resonance analysis. Genes. Cells 15, 269-280 (2010). https://doi.org/10.1111/j.1365-2443.2009.01377.x
[31] Nishiwaki, T., Satomi, Y., Nakajima, M., Lee, C., Kiyohara, R., Kageyama, H., et al. Role of KaiC phosphorylation in the circadian clock system of Synechococcus elongatus PCC 7942. Proc. Natl. Acad. Sci. U.S.A. 101, 13927-13932 (2004). https://doi.org/10.1073/pnas.0403906101
[32] Kuligowski, J., Carrión, D., Quintás, G., Garrigues, S., de la Guardia, M. Cubic smoothing splines background correction in on-line liquid chromatography-Fourier transform infrared spectrometry. J. Chromatogr. A 1217, 6733-6741 (2010). https://doi.org/10.1016/j.chroma.2010.05.033
[33] Busnel, J. P., Foucault, F., Denis, L., Lee, W., Chang, T. Investigation and interpretation of band broadening in size exclusion chromatography. J. Chromatogr. A 930, 61-71 (2001). https://doi.org/10.1016/s0021-9673(01)01159-1
[34] Furuike, Y., Abe, J., Mukaiyama, A., Akiyama, S. Accelerating *in vitro* studies on circadian clock systems using

an automated sampling device. Biophys. Physicobiol. 13, 235-241 (2016). https://doi.org/10.2142/biophysico.13.0_235
[35] Mutoh, R., Nishimura, A., Yasui, S., Onai, K., Ishiura, M. The ATP-mediated regulation of KaiB-KaiC interaction in the cyanobacterial circadian clock. PLoS One 8, e80200 (2013). https://doi.org/10.1371/journal.pone.0080200
[36] Phong, C., Markson, J. S., Wilhoite, C. M., Rust, M. J. Robust and tunable circadian rhythms from differentially sensitive catalytic domains. Proc. Natl. Acad. Sci. U.S.A. 110, 1124-1129 (2013). https://doi.org/10.1073/pnas.1212113110
[37] Abe, J., Hiyama, T. B., Mukaiyama, A., Son, S., Mori, T., Saito, S., et al. Circadian rhythms. Atomic-scale origins of slowness in the cyanobacterial circadian clock. Science 349, 312-316 (2015). https://doi.org/10.1126/science.1261040
[38] Ouyang, D., Furuike, Y., Mukaiyama, A., Ito-Miwa, K., Kondo, T., Akiyama, S. Development and optimization of expression, purification, and ATPase assay of KaiC for medium-throughput screening of circadian clock mutants in cyanobacteria. Int. J. Mol. Sci. 20, 2789 (2019). https://doi.org/10.3390/ijms20112789
[39] Terauchi, K., Kitayama, Y., Nishiwaki, T., Miwa, K., Murayama, Y., Oyama, T., et al. ATPase activity of KaiC determines the basic timing for circadian clock of cyanobacteria. Proc. Natl. Acad. Sci. U.S.A. 104, 16377-16381 (2007). https://doi.org/10.1073/pnas.0706292104
[40] Pittendrigh, C. S. On temperature independence in the clock system controlling emergence time in drosophila. Proc. Natl. Acad. Sci. U.S.A. 40, 1018-1029 (1954). https://doi.org/10.1073/pnas.40.10.1018
[41] Blandamer, M. J., Morris, S. H. Investigation into effect of temperature and added tert-butyl alcohol on dynamic properties of belousov reaction. J. Chem. Soc. Farad. 71, 2319-2330 (1975). https://doi.org/10.1039/f19757102319
[42] Karr, T. L., Kristofferson, D., Purich, D. L. Mechanism of microtubule depolymerization - Correlation of rapid induced disassembly experiments with a Kinetic-model for endwise depolymerization. J. Biol. Chem. 255, 8560-8566 (1980). https://doi.org/10.1016/S0021-9258(18)43534-X
[43] Kasai, R. S., Suzuki, K. G. N., Prossnitz, E. R., Koyama-Honda, I., Nakada, C., Fujiwara, T. K., et al. Full characterization of GPCR monomer-dimer dynamic equilibrium by single molecule imaging. J. Cell Biol. 192, 463-480 (2011). https://doi.org/10.1083/jcb.201009128
[44] Pollard, T. D. Rate constants for the reactions of Atp-actin and Adp-actin with the ends of Actin-filaments. J. Cell Biol. 103, 2747-2754 (1986). https://doi.org/10.1083/jcb.103.6.2747
[45] Miyoshi, T., Tsuji, T., Higashida, C., Hertzog, M., Fujita, A., Narumiya, S., et al. Actin turnover-dependent fast dissociation of capping protein in the dendritic nucleation actin network: evidence of frequent filament severing. J. Cell Biol. 175, 947-955 (2006). https://doi.org/10.1083/jcb.200604176
[46] Kriegenburg, F., Seeger, M., Saeki, Y., Tanaka, K., Lauridsen, A. M. B., Hartmann-Petersen, R., et al. Mammalian 26S proteasomes remain intact during protein degradation. Cell 135, 355-365 (2008). https://doi.org/10.1016/j.cell.2008.08.032
[47] Ip, S. H. C., Ackers, G. K. Thermodynamic studies on subunit assembly in human hemoglobin - Temperature-dependence of dimer-tetramer association constants for oxygenated and unliganded hemoglobins. J. Biol. Chem. 252, 74-81 (1977). https://doi.org/10.1016/S0021-9258(17)32800-4
[48] Ito-Miwa, K., Furuike, Y., Akiyama, S., Kondo, T. Tuning the circadian period of cyanobacteria up to 6.6 days by the single amino acid substitutions in KaiC. Proc. Natl. Acad. Sci. U.S.A. 117, 20926-20931 (2020). https://doi.org/10.1073/pnas.2005496117
[49] Furuike, Y., Mukaiyama, A., Koda, S., Simon, D., Ouyang, D., Ito-Miwa, K., et al. Regulation mechanisms of the dual ATPase in KaiC. bioRxiv (2021). https://doi.org/10.1101/2021.10.28.466029